Water and Environment Journal
Promoting Sustainable Solutions

Water and Environment Journal. Print ISSN 1747-6585

Numerical investigation of the effects of combining sewer junction characteristics on the hydraulic parameters of flow in fully surcharged condition

Yaser Yekani Motlagh[1], Amir H. Nazemi[1], Ali A. Sadraddini[1], Akram Abbaspour[1] & Saber Yekani Motlagh[2]

[1]School of Water Engineering, Tabriz University, Tabriz, Iran and [2]School of Mechanical Engineering, Urmia University of Technology (UUT), Urmia, Iran

Keywords
energy loss; flow structure; manhole; sewer junction.

Correspondence
Yaser Yekani Motlagh, School of Water Engineering, Tabriz University, Tabriz 0098, Iran. Email: Y_Y_motlagh@yahoo.com

doi:10.1111/j.1747-6593.2012.00347.x

Abstract

In this study, the effects of different parameters on flow structure and flow hydraulics for combining sewer junction consisting of manhole and lateral inflow were investigated numerically. For this purpose, the effects of dimension variations, main and lateral pipe slope, angle and the joint position of lateral pipe beside manhole, manhole geometry, and the outflow rate of manhole on flow structure and energy loss coefficients were investigated. Results show that the rate of energy loss decreases by heightening the installation position of lateral pipe beside manhole. In addition, it was shown that the slope variations of main and lateral pipes and outflow rate do not affect the rate of energy loss.

Introduction

Sewer junctions are principal components of drainage systems, as they connect pieces of sewer pipes to form sewer networks. Understanding the hydraulics of sewers at the junctions is important as these junctions usually become the bottlenecks of the sewer systems. Junctions combining lateral inflows at different angles with the straight-through flow are of particular interest as they are the most widely used junctions in the sewer systems.

Flows in angulated junctions present complicated patterns of waves, mixing, separation, turbulence, and the transition between, or the coexistence of, open-channel flow and full-pipe flow. Full-pipe flow, also referred as surcharged flow, occurs when the carrying capacity of the sewer system is exceeded. Although weakly surcharged flows are allowed in the sewer design as a compromise between the flow-carrying capacity and economy, strongly surcharged flows could cause serious problems, such as blown-off manhole covers, sewer pipe rupture, flooding and soil erosion. Surcharged flows may be avoided by increasing the size and slope of the sewer pipes to gain more carrying capacity; however, in many cases, sewer junctions form the bottlenecks of the sewer network and cause the surcharged flow. For example, Zhao *et al*. (2004) reported a surcharged flow caused by a 90° junction in Calgary, Alberta, where the manhole cover was blown off and a large fountain was formed. In such cases, the hydraulic performance of the sewer junction must be understood to increase the capability of the sewer network.

To determine the discharge capacity of a network, the major head loss and also the hydraulic characteristics of the fitting components and their minor head losses should be evaluated properly. Fittings and junctions, because of their local head losses, produce a back water effect (Yen & Akan 1999) and influence the discharge capacity by increasing the water surface elevation in free surface flow networks. Therefore, the existence of uncertainty in the hydraulic characteristics of junctions, manholes and other fittings would significantly affect the determination of the discharge capacity of a network, and should be avoided. In this regard, the available information related to open-channel flow junctions is mostly on rectangular cross-sections. The huge volume of research on this subject during the last five decades has covered topics such as the depth ratio between the upstream branches and the downstream channel (Taylor 1944; Hsu *et al*. 1998a; Gurram & Karki 2000), characteristics of the separation zones (Best & Reid 1984; Hsu *et al*. 1998b, 2002), velocity patterns and shear stress distributions (Joy & Townsend 1981), presence of supercritical flow and hydraulic jumps (Hager 1989), energy and momentum correction factors (Joy & Townsend 1981; Hsu *et al*. 1998b), effect of bed discordance on the channel junction flow (Biron *et al*. 1996), and the head losses in various geometries and hydraulic circumstances (Webber & Greated 1966; Lin & Soong 1979; Hsu *et al*. 1998a, 2002; Gurram and Karki, 2000). Moreover,

detailed information regarding 3D flow patterns in rectangular open-channel flow junctions have been presented in some researches (Ramamurthy *et al*. 2007; Weber *et al*. 2001; Huang *et al*. 2002). Also, a large number of experimental studies presented various energy loss coefficients for flows passing the junctions of closed pipes in a pressurised flow regime (McNown 1954; Gardel 1957a,b; Sangster *et al*. 1958, 1961; Blaisdell & Manson 1963; Ito & Imai 1973; Lindvall 1984, 1987; Johnston & Volker 1990; Miller 1990; Serre *et al*. 1994; Ramamurthy & Zhu 1997). These tests were conducted for different branches and main diameter ratios, and for different pipe alignments.

Manholes are also necessary components in a drainage network. The hydraulic behaviour of these structures was mainly investigated for sewer and urban drainage networks in which the longitudinal slope range is usually greater than that employed in agricultural drainage systems. Methods of classification of sewer junctions have been summarised by Yen (1986). Also, the subject of energy loss in manholes has been investigated by various researchers (Ackers 1959; Howarth & Saul 1984; Marsalek 1984, 1985; Johnston & Volker 1990; Sakakibari *et al*. 1997; Wang *et al*. 1998).

Recently, Bayat *et al*. (2010) experimentally determined the major head loss of corrugated pipes and the local head loss coefficients for different junctions and manholes.

Also, aided by an expanded knowledge on flow regimes in sewer junctions, and specifically on surcharged junction flows, the combined supercritical flows in these junctions have been studied by many researchers (Del Giudice *et al*. 2000; Del Giudice & Hager 2001; Gargano & Hager 2002; Gisonni & Hager 2002; Zhao *et al*. 2004, 2006, 2008).

Today, owing to the advances in computational fluid dynamics (CFD) and computing power, the CFD method is commonly used in hydraulic researches as an alternative or complementary approach to laboratory experimentation. The use of CFD modelling in sewer junction studies has many advantages compared with the physical model studies. First of all, CFD modelling is usually cost-effective, efficient and free of scale effects. A verified CFD model can be used as a design tool to optimise sewer junction designs. The capabilities of CFD modelling in providing flow structure details (e.g. velocity distributions, turbulence, flow separation and mixing in sewer junctions) can be tremendously useful. These details are not only important in optimising sewer junctions' designs, but also essential for understanding the subject of sediment transport in sewers. This is very important because of providing its relation with build-up of sedimentation in sewers and its effect on water quality (Stein *et al*. 1999; Guymer & O'Brien 2000). Marsalek (1985) and Zhao *et al*. (2008) have investigated the influence of manhole dimensions on energy loss. According to the experimental works of Marsalek and the simulations of Zhao about the study of energy loss on square manholes with the dimensions of (2–5)D, it has been shown that energy loss and water depth increase by increasing manhole dimensions. This increment is considerable up to 3D case where k increases from 0.59 to 0.81. But for dimensions higher than 3D, the variation of manhole depth by increasing manhole dimensions will be negligible. Also, the rate of energy loss variations will be 5% up to 5D case.

In this research, a fully surcharged flow at different merging angles was studied. The studied junction has two inflows and one outflow. All three connecting pipes run full with a free surface in the junction chamber (fully surcharged flow). The main objectives of the present study were as follows: (1) providing details of the flow structure in 90° junction, and validating the obtained results with the available experimental and numerical data; (2) investigating the flow structure and hydraulic performance of sewer junctions with various merge angles; and (3) investigating the effects of manhole shapes on the hydraulic function and flow structure.

Geometry, boundary conditions and hydraulic parameters

The present study has investigated fully surcharged flow at a junction that combines pipes connected as shown in Fig. 1, (for $\theta = 90°$). The junction has three connecting pipes running full, and the lateral inlet pipe is laid out at θ to the other two pipes. The straight inflow, lateral inflow and the outflow are denoted as Q_1, Q_2 andQ_3, respectively.

All connecting pipes have an identical diameter of D = 0.152 m. The junction chamber is a rectangular box with a length and width of 3D and 2D, respectively. The inlet and outlet pipes are located 5 cm and 4 cm above the bottom of the junction chamber, respectively. The lengths of straight inflow, lateral inflow and outflow pipes are 2.0, 3.8 and 2.0 m, respectively.

The hydraulic parameters used in the sewer design include the mean water depth (h_m) in the junction chamber, and the energy coefficients. The energy loss coefficients at the combining sewer junctions are usually defined as (Marsalek 1985; Wang *et al*. 1998; Zhao *et al*. 2006):

$$k = \frac{Q_1}{Q_3}k_{13} + \frac{Q_2}{Q_3}k_{23} \quad k_{23} = \frac{H_2 - H_3}{v^3/2g} \quad k_{13} = \frac{H_1 - H_3}{v^3/2g} \qquad (1)$$

where $H_i = \frac{v_i^2}{2g} + \frac{p_i}{\rho g}$ and the average velocity in the outlet pipe is $V_3 = Q_3/A_3$. K_{13} and K_{23} denote energy changes in the straight and lateral streams, respectively. K is the head loss coefficient.

As shown in Fig. 1, the simulation domain has two inlets (Q_1 and Q_2) for which uniform velocities are assigned, assuming a turbulent intensity of 3.7% and an eddy length scale of $D/4$(Zhao *et al*. 2008). In the outlet pipe, atmospheric pressure is assumed over the outlet boundary (Q_3). An inlet–outlet boundary condition is applied to the top of the chamber with

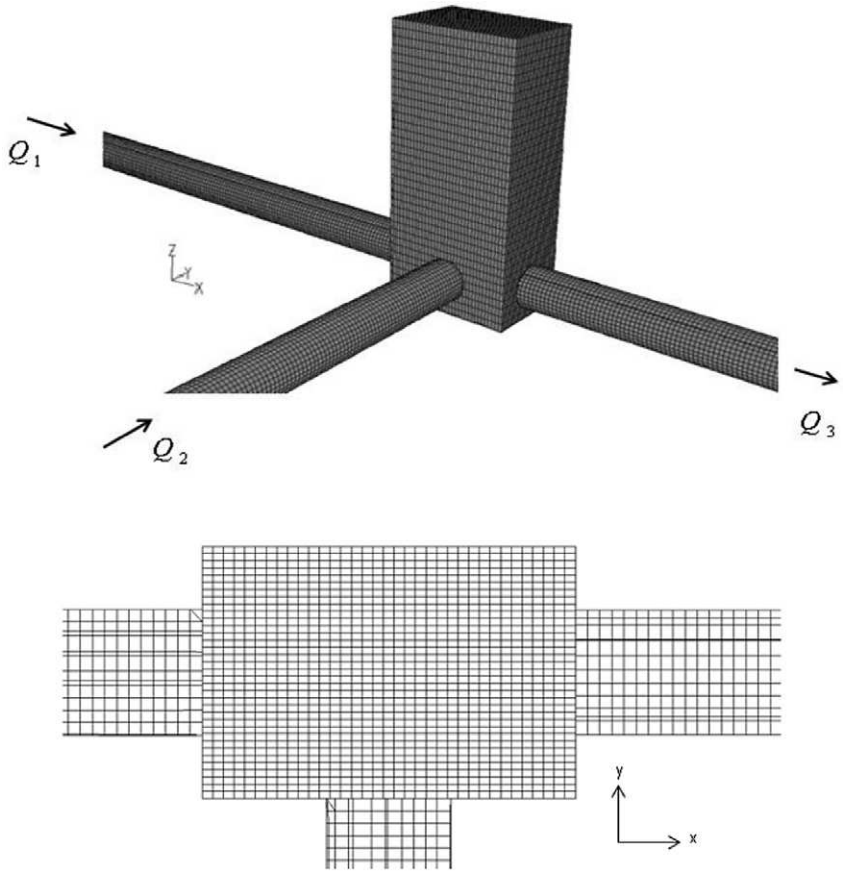

Fig. 1. Geometry, mesh configuration.

Table 1 Different numbers of network elements for the sensitivity analysis step

Mesh number	Mesh 1	Mesh2	Mesh 3	Mesh4	Mesh5	Mesh6	Mesh7
Number of cells	30 744	42 728	52 152	89 422	134 091	169 019	205 687
Number of nodes	37 042	50 175	60 283	102 412	150 617	187 845	227 557

a relative pressure equal to the atmospheric pressure, which allows the air to cross the boundary either into or out of the domain.

In the present research work, angle values of $\theta = 30°$, 45°, 60°, 75°, 90° have been investigated. At each angle, hydraulic parameters and flow structures were compared for flow ratios of $Q_2/Q_3 = 0.2$, 0.4, 0.5, 0.7, where $Q_3 = 0.035\ m^3/s$.

Mesh study

The applied mesh contained structured grids as shown in Fig. 1.

In this investigation, the mesh sensitivity analysis was performed for all cases, and the number of meshes selected for the numerical calculations was 169 019. In this section, for flow ratio of $Q_2/Q_3 = 0.7$and merge angle of $\theta = 90°$, the sensitivity analysis was performed using different numbers of mesh network elements, according to Table 1.

To investigate the network sensitivity, changes of the average relative error for the energy loss coefficients of $K_{13}K_{23}K$ were explored. According to the obtained results shown in Fig. 2, the solution becomes mesh-independent at the number of elements equal to 134 091. Thus, by considering mesh networks in other circumstances, 169 019 mesh elements were finally selected for the simulations.

Numerical solution of governing equations

The governing equations comprised the time-averaged three-dimensional momentum (Navier–Stokes) equation, the energy equation, continuity equations, the transport equa-

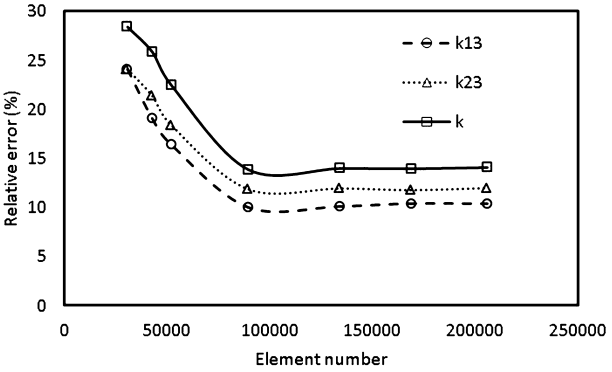

Fig. 2. Mesh sensitivity analysis.

tion of volume fraction related to volume of fluid (VOF) method, and the equations of the turbulence model.

In the Reynolds-averaged approach to turbulence, the unsteadiness is averaged out; in fact, unsteadiness is regarded as part of turbulence. Equation (2) denotes the Reynolds-averaged Navier–Stokes (RANS) equation, i = 1, 2, 3, and j = 1, 2, 3 (Anderson *et al*. 1997).

$$\frac{\partial U_i}{\partial t}+U_j\frac{\partial U_i}{\partial x_j}=-\frac{\partial P}{\partial x_i}+\frac{\partial}{\partial x_j}\left[\nu\left(\frac{\partial U_i}{\partial x_j}+\frac{\partial U_j}{\partial x_i}\right)-\overline{u_iu_i}\right] \quad (2)$$

where g is the acceleration because of gravity; p is the pressure; t is time; U_i is the mean velocity in different directions; and u_i is the fluctuating part of velocity.

Also, the continuity equation is as follows:

$$\frac{\partial U_i}{\partial x_i}=0 \quad (3)$$

The two-equation turbulence models are based on the Boussinesq eddy-viscosity approximation, which assumes that the principal axes of the Reynolds stress tensor τ_{ij} are coincident with those of the mean strain-rate tensor $S_{ij}=\frac{1}{2}\left(\frac{\partial U_i}{\partial x_j}+\frac{\partial U_j}{\partial x_i}\right)$ at all points in a turbulent flow. This is analogous to the Stokes postulate for laminar flows. The coefficient of proportionality between τ_{ij} and S_{ij} is eddy viscosity ν_T (Anderson *et al*. 1997).

$$\tau_{ij}=-\overline{u_iu_i}=\nu_TS_{ij}-\frac{2}{3}k\delta_{ij} \quad (4)$$

δ_{ij} is the Kronecker delta function, and k is the mean turbulence kinetic energy. The two-equation models are the most popular turbulence models in numerical simulation of turbulent flows.

For two-phase flow simulations, the VOF scheme is widely used. For the VOF scheme, one has to introduce a new variable c, which is called the void fraction. The void fraction c is defined by the ratio of water to air in a cell. Generally, c = 1 when the cell is full of water, and c = 0 when the cell is full of air. The governing equation of c is as follows (Hirt & Nichols 1992):

$$\frac{\partial c}{\partial t}+\frac{\partial}{\partial x_j}(U_jc)=0 \quad (5)$$

Also, c must satisfy the condition $0 < c < 1$.

For free-surface problems, one has to solve the equation for the void fraction along with the conservation equation for mass and momentum. Alternatively, near the free-surface boundary, one can treat both fluids as a single fluid whose properties vary in space according to the volume fraction of each phase, as follows (Hirt & Nichols 1992):

$$\rho=\rho_1c+\rho_2(1-c) \quad (6)$$

$$\mu=\mu_1c+\mu_2(1-c) \quad (7)$$

where $\rho(kg/m^3)$ is density and $\mu(N/m^2)$ is molecular viscosity. Subscripts 1 and 2 denote the two fluids (e.g. water and air).

In this paper, the open source CFD package, Open Source Field Operation and Manipulation ('OpenFOAM'), which is based on the work of Weller *et al*. (1998), was used for the flow simulation.

The discretisation of the flow governing equations in the 'OpenFOAM' is based on the finite volume method formulated with the collocated variable arrangement, with the pressure and velocity solved by segregated methods. OpenFOAM is a C++ code library of classes for writing CFD codes, which includes a well-tested and validated RANS capability, and the VOF model for the two-phase flow modelling. Several numerical convection differencing schemes are available in OpenFOAM, including upwind, central difference, QUICK and flux limiters schemes. In this work, the limited linear differencing scheme (limited linear V) (Jasak *et al*. 1999) was used. It is a bounded high-order scheme that takes into account the direction of the flow field. For the first time derivative, the choice is the Euler implicit first order. The set of discretised equations were solved by the algebraic multigrid solver (for pressure), and by the incomplete Cholesky preconditioned biconjugate gradient (BICCG) solver (for the rest of the variables).

Then, different cases listed in Table 2 were executed to determine the appropriate algorithm for the velocity-pressure coupling and the turbulence model.

The resulting average relative errors of energy loss coefficients obtained from various models were compared with the experimental results presented by Zhao *et al*. (2006) in Fig. 3.

Based on the obtained results, it can be concluded that case 3, which includes the pressure implicit with split operator (PISO) algorithm along with the $k-\omega$ turbulence model,

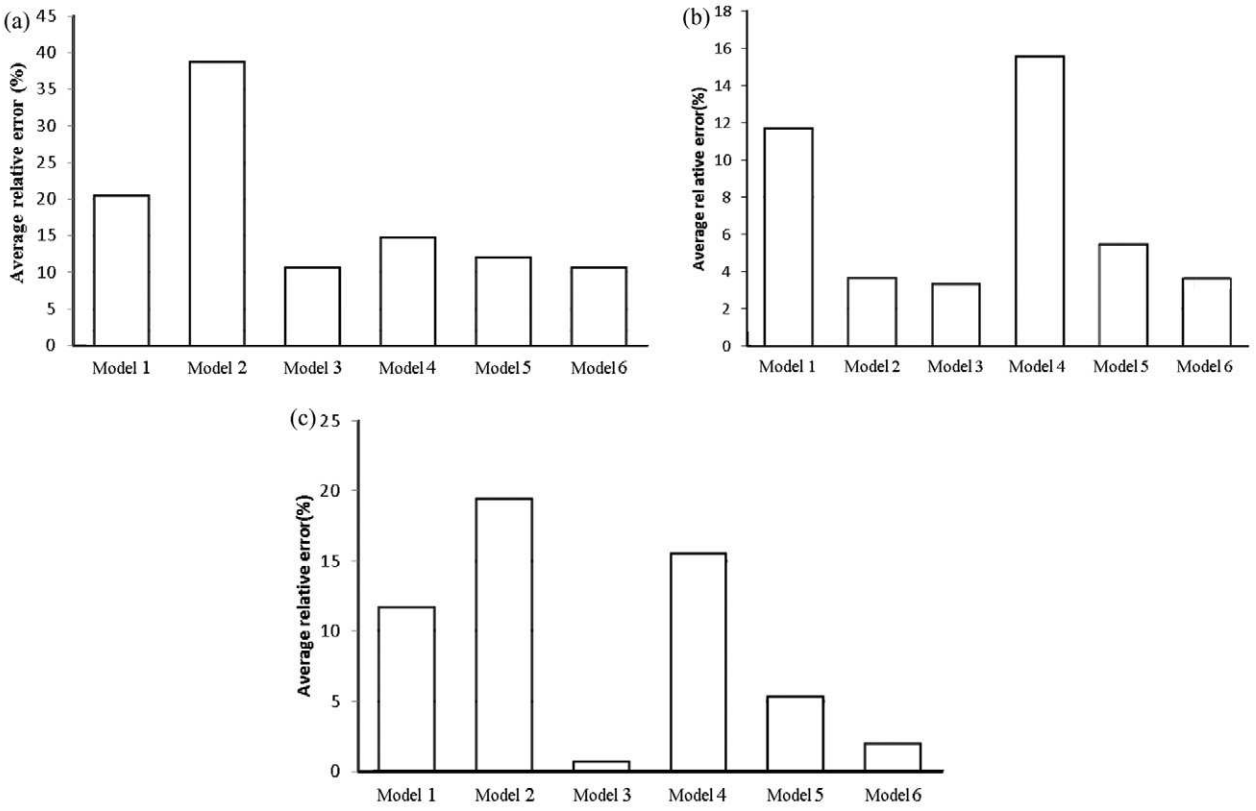

Fig. 3. Average relative error for (a) K_{13}; (b) K_{23}; (c) K.

Table 2 Various algorithms and turbulence models

Case	Turbulence model	Pressure-velocity coupling
1	k-ε/Standard	PISO
2	k-ε/RNG	PISO
3	$k-\omega$	PISO
4	k-ε/Realisable	PISO
5	$k-\omega$	SIMPLEC
6	$k-\omega$	SIMPLE

has a better performance to predict the energy loss coefficients compared with the other combinations.

Energy loss coefficients and water depth in a junction chamber with a lateral pipe connected at 90°

Figure 4 shows the energy loss coefficients and water depth at various flow rates in a junction chamber with a lateral pipe connected at 90°. The numerical results of the present work (VOF model) were compared with the experimental results of Zhao *et al*. (2008). Their method was used for modelling two-fluid homogeneous and inhomogeneous flows.

As it can be observed in Fig. 4, the numerical results of the present research have a good consistency with the experimental results. In addition, the VOF method shows a better performance to predict the water depth and energy loss coefficients in a junction chamber compared with the homogeneous and inhomogeneous models.

Effect of change of merge angle and flow rate on the hydraulic parameters and structure of the flow in a junction chamber

In this section, the variations of energy loss coefficients and average water depth in a junction chamber were investigated by changing the connection angle of the lateral pipe. In addition, the factors influencing the hydraulic parameters were studied by determining the flow pattern inside the junction chamber.

Energy loss coefficients and water depth in the junction chamber

The energy loss coefficients and water depth in a junction chamber at various flow rates and pipe merge angles of $\theta = 30°$, 45°, 60°, 75°, 90° were presented in Fig. 5.

It was observed that increasing the ratio of lateral flow rate to outlet flow rate (Q_2/Q_3) at a fixed connection angle

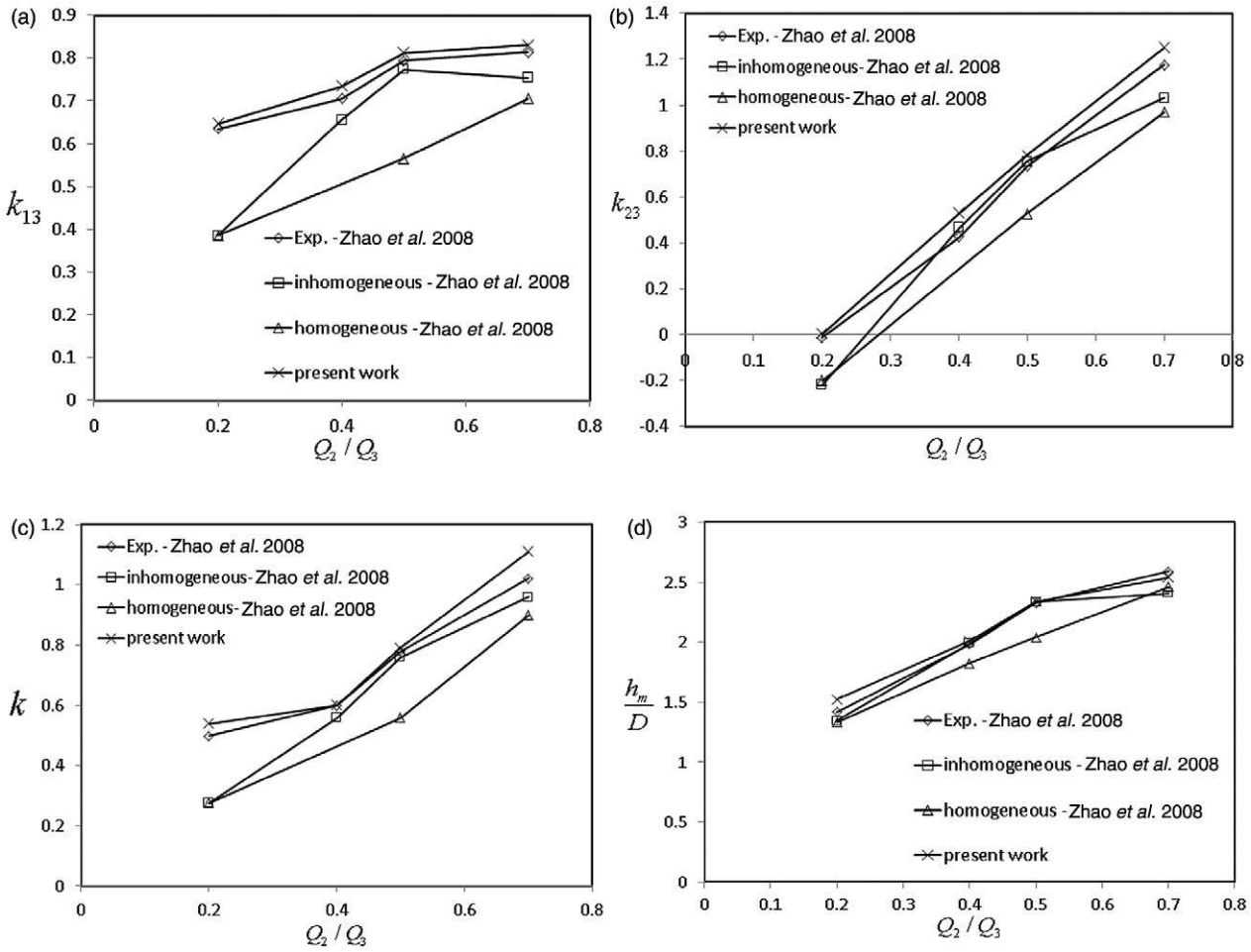

Fig. 4. Comparison of numerical simulation results of the present work with the numerical and experimental results of Zhao *et al*. (2008): (a) k_{13}; (b) k_{23}; (c) k; (d) $\frac{h_m}{D}$.

increases the energy loss coefficients and water depth in the junction chamber. Moreover, increasing the merge angle of the lateral pipe at high flow ratios increases the energy loss coefficients and water depth. The main causes of energy loss at the connections and junctions are vortical flows, sudden change of flow direction and flow separation.

In the flows containing suspended particles, the created vortices entrap these particles. Later, these particles settle to the bottom of the junction chamber. The sedimentation of these suspended solids will lead to the clogging of the junction chamber and the disruption of the flow inside; therefore, knowing the details of the flow structure could be useful.

Review of flow structure

The inflow of fluid through the angled lateral pipes into the junction chamber causes the creation of complex vortical patterns inside the chamber. To determine the flow structure in the junction chamber, the velocity vectors for different flow ratios and connection angles of pipes have been illustrated in Fig. 6.

For all the merge angles, at the flow ratio of $Q_2/Q_3 = 0.2$ (Fig. 6a,c,e), the straight inflow is dominant; and the lateral inflow has little effect on the straight flow direction. On the other hand, the lateral flow goes through a rotation until exiting the junction chamber in the *x* direction. Moreover, in the upper section of the junction chamber, a long and thin vortex is created along the chamber wall, and a small circular vortex forms in the lower left corner.

When the flow ratio is $Q_2/Q_3 = 0.7$(Fig. 6b,d,f), the lateral flow dominates. This flow cuts off the straight inflow, runs into the junction chamber wall with a little bend, and then spreads. As a result of the impact of these two inflows, a strong vortical flow is formed in the upper left corner of the junction chamber, which causes a large reduction in the flow

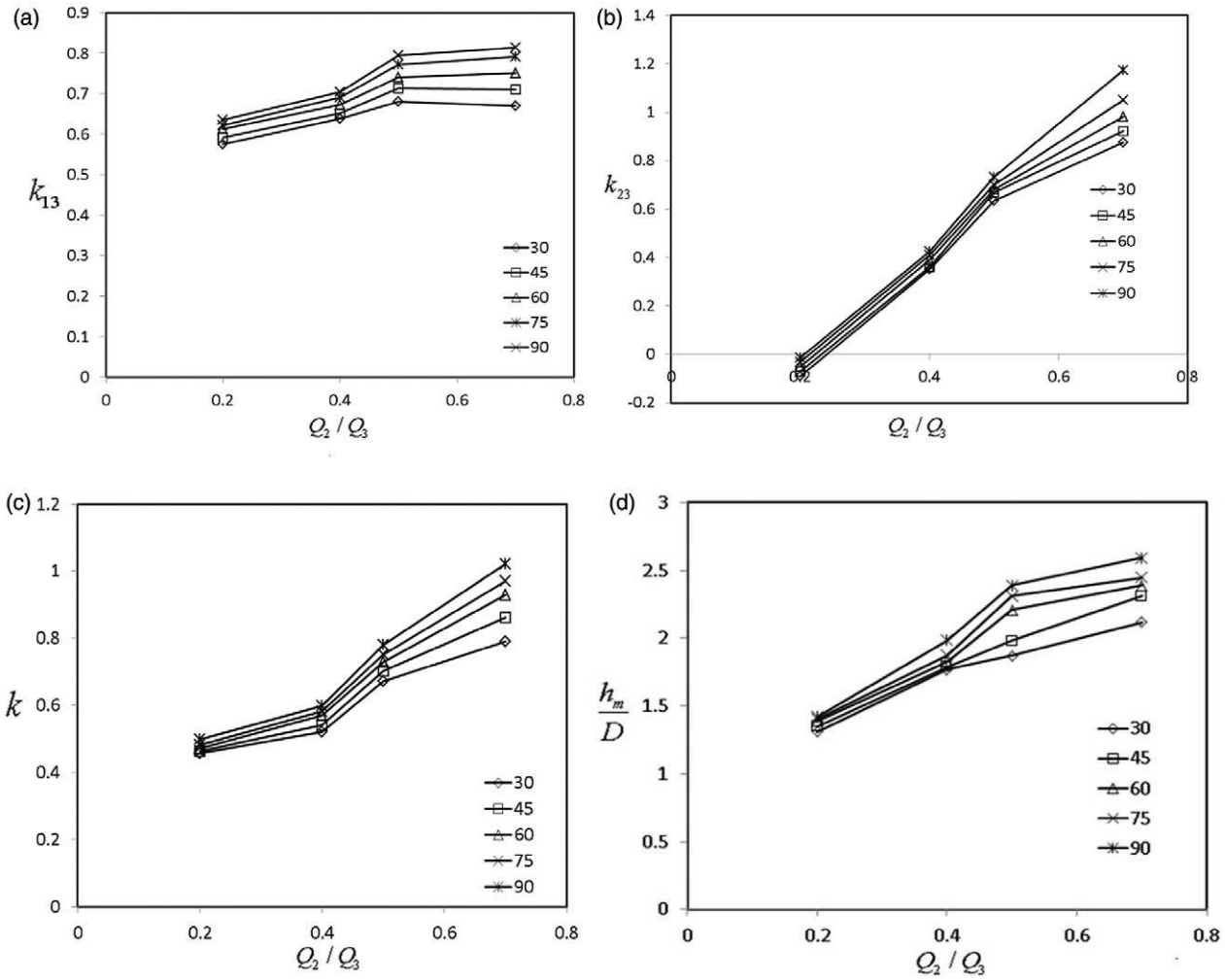

Fig. 5. Water depths and energy loss coefficients in the junction chamber for various merge angles: (a) k_{13}; (b) k_{23}; (c) k; (d) $\frac{h_m}{D}$.

energy. Also, the small circular vortex in the lower left corner of the junction chamber intensifies.

A review of the flow structures at various flow ratios shows that, as this ratio gets smaller, the resulting thin and long vortical and secondary flows will have less intensity, and as this ratio gets larger, the vortical flow intensity increases. As a result, increasing the flow ratio (Q_2/Q_3) increases the flow energy loss and the water depth in the junction chamber. This trend can be observed in the results of Fig. 5.

At the 30° merge angle, the straight flow is less affected by the flow in the lateral pipe because the angle between the lateral pipe and the straight flow is small (Fig. 6a,b). In this situation, there is a thin vortex in the upper part of the junction chamber, and a small vortex in the lower left corner.

At the large flow ratio of $Q_2/Q_3 = 0.7$, by increasing the merge angle, the effect of the lateral flow on the straight flow increases. In this case, as it can be seen in Fig. 6(d), the weak and thin vortex in the upper part of the junction chamber transforms into the strong circular vortex in the upper left corner.

With the increase of the merge angle to 90°, at the large flow ratio of $Q_2/Q_3 = 0.7$ (Fig. 6f), the straight flow is completely deviated by the lateral flow. In this condition, a large portion of the junction chamber becomes vortical.

At the small flow ratio of $Q_2/Q_3 = 0.2$, as the flow in straight pipe is dominant, the flow pattern does not change considerably by increasing the merge angle of the lateral pipe (Fig. 6a,c,e).

Therefore, it can be stated that changing the merge angle at large flow ratios ($\frac{Q_2}{Q_3} > 0.6$) strongly affects the flow structure where the lateral flow is dominant. However, at small

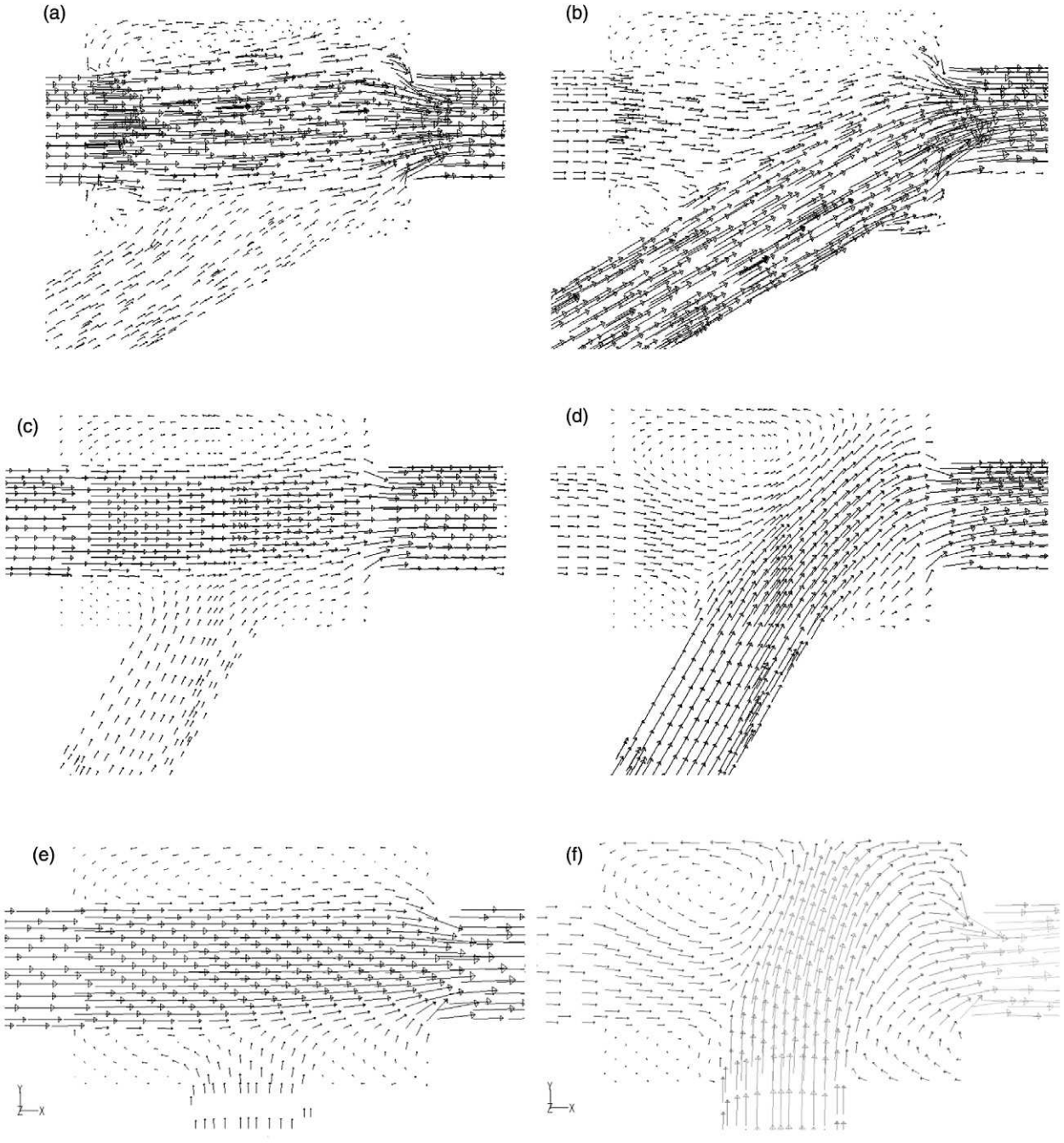

Fig. 6. Velocity vectors inside the junction chamber for different merge angles of lateral pipes on the horizontal plane Z/D = 0.8: (a) $\theta = 30°$, $Q_2/Q_3 = 0.2$; (b) $\theta = 30°$, $Q_2/Q_3 = 0.7$; (c) $\theta = 60°$, $Q_2/Q_3 = 0.2$; (d) $\theta = 60°$, $Q_2/Q_3 = 0.7$; (e) $\theta = 90°$, $Q_2/Q_3 = 0.2$; (f) $\theta = 90°$, $Q_2/Q_3 = 0.7$. (Arrow length indicates the magnitude of velocity).

flow ratios ($\frac{Q_2}{Q_3} < 0.4$), the flow pattern inside the junction chamber does not change considerably with the change of the connection angle. Thus, as shown in Fig. 5, at low flow rates (e.g. $Q_2/Q_3 = 0.2$), the energy loss coefficients are almost the same at different merge angles; while at high flow rates (e.g. $Q_2/Q_3 = 0.7$), increasing the merge angle increases the energy loss coefficients as a larger portion of the flow becomes vortical.

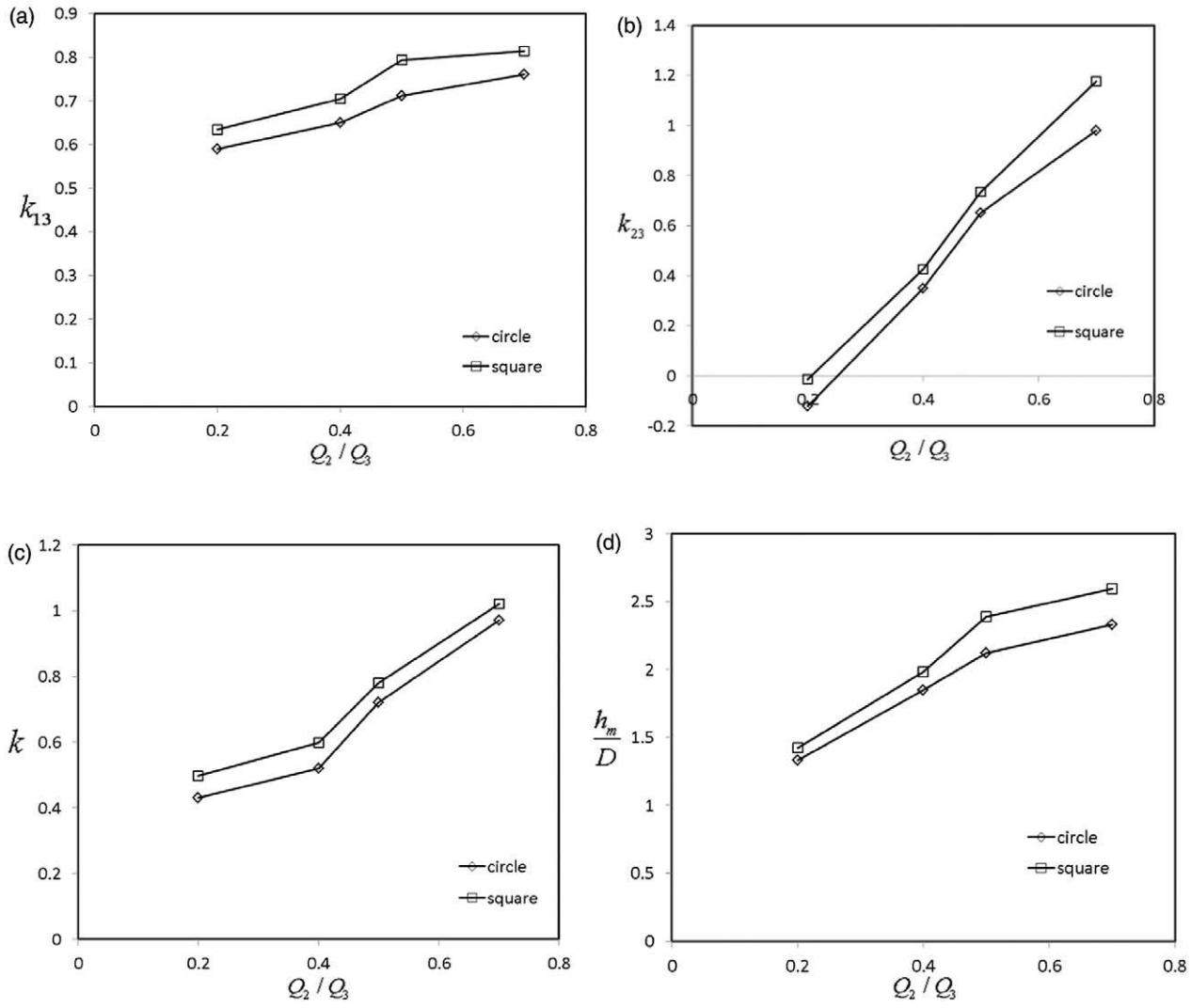

Fig. 7. Comparison of energy loss coefficients and water depths in junction chambers with rectangular and circular cross-sections: (a) k_{13}; (b) k_{23}; (c) k; (d) $\frac{h_m}{D}$.

Effect of change of junction chamber geometry on the hydraulic parameters and structure of the flow

In this section, by changing the cross-section of the junction chamber from rectangular to circular, the hydraulic parameters and flow structure were studied. The areas of rectangular and circular cross-sections were assumed to be identical. The problem was solved for the case of a 90° merge angle and flow rate ratios of $Q_2/Q_3 = 0.2, 0.4, 0.5, 0.7$.

Energy loss coefficients and water depth in the junction chamber

In Fig. 7, the values of energy loss coefficients and water depths in the junction chambers with rectangular and circular cross-sections were compared in various flow rates.

As it can be observed, the energy loss coefficients and water depths at all studied flow rates for the junction chamber with the circular cross-section were less than the one with the rectangular cross-section. In order to explore the underlying causes, the flow structures in the two cases were examined in the following section.

Review of flow structure

The velocity vectors in the junction chambers with rectangular and circular cross-sections have been illustrated in Fig. 8.

It can be observed that the existing flow structures for both cases are the same, meaning that, for both types of

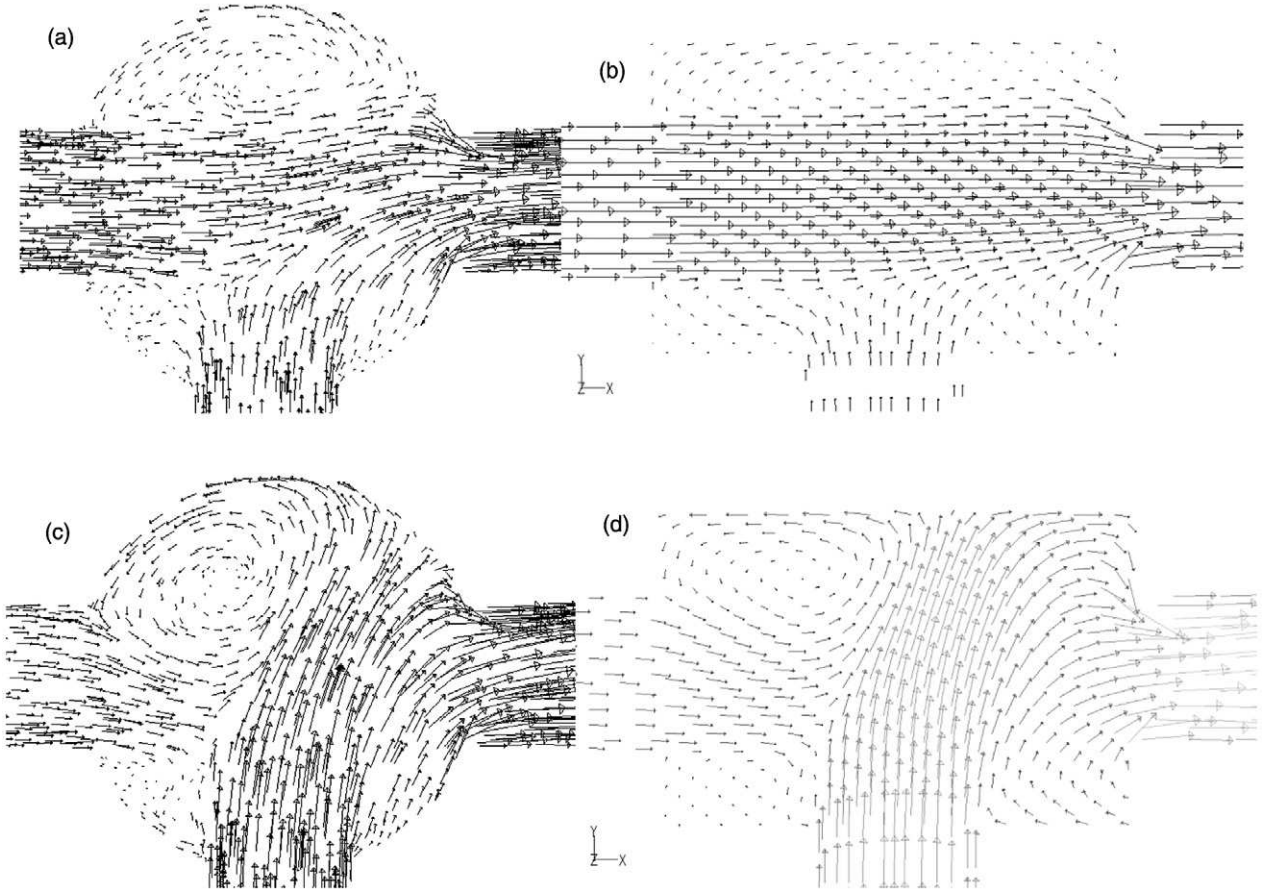

Fig. 8. Velocity vectors inside the junction chamber on the horizontal plane Z/D = 0.8: (a) circular cross-section, $Q_2/Q_3 = 0.2$; (b) rectangular cross-section, $Q_2/Q_3 = 0.2$; (c) circular cross-section, $Q_2/Q_3 = 0.7$; (d) rectangular cross-section, $Q_2/Q_3 = 0.7$. (Arrow length indicates the magnitude of velocity).

cross-sections, at small flow ratios (Q_2/Q_3), a weak and thin vortex forms in the upper part of the junction chamber, which at large flow ratios, turns into a strong circular vortex in the upper left corner. In addition, at both small and large flow rate ratios, a small and weak vortex is generated in the lower left corner. In addition, there are no sharp corners in the cylindrical junction chamber, and the curvature of the wall prevents sudden direction changes, which is one of the causes of energy loss in the flow.

Effect of change of position of lateral pipe on the hydraulic parameters and structure of the flow

In this part, the effect of heightening the installation position of the lateral pipe beside manhole on flow structure and energy loss was studied. For this purpose, lateral pipe is studied for different distances between pipe and manhole like 5, 10, 15 and 20 cm. Also, the flow structure was studied for the angle of 90° in different flow rates.

For different positions of lateral pipe, the loss of energy coefficients in different flow rate ratios was shown in Fig. 9.

Results show that the value of k_{13} decreases by increasing the height. Flow modelling inside the manhole for Z/D = 0.8 was shown in Fig. 10 to investigate the reason.

It was shown that the interaction between main and lateral flows decreases by increasing the height, which decreases vortical flows and flow turbulence. This decreases energy loss in the main flow path. The investigation of energy loss coefficient, k_{23}, revealed that vortical flow and energy loss increase by increasing the height. It can be deduced that the total loss or k coefficient decreases in manhole by increasing the height.

Effect of pipe diameter on the hydraulic parameters and flow structure

In this part, the effect of the main and lateral pipes diameters was investigated on energy loss and flow modelling. For this purpose, the problem was studied for $D_1 = 0.75D_3$, $D_2 = 0.5D_3$

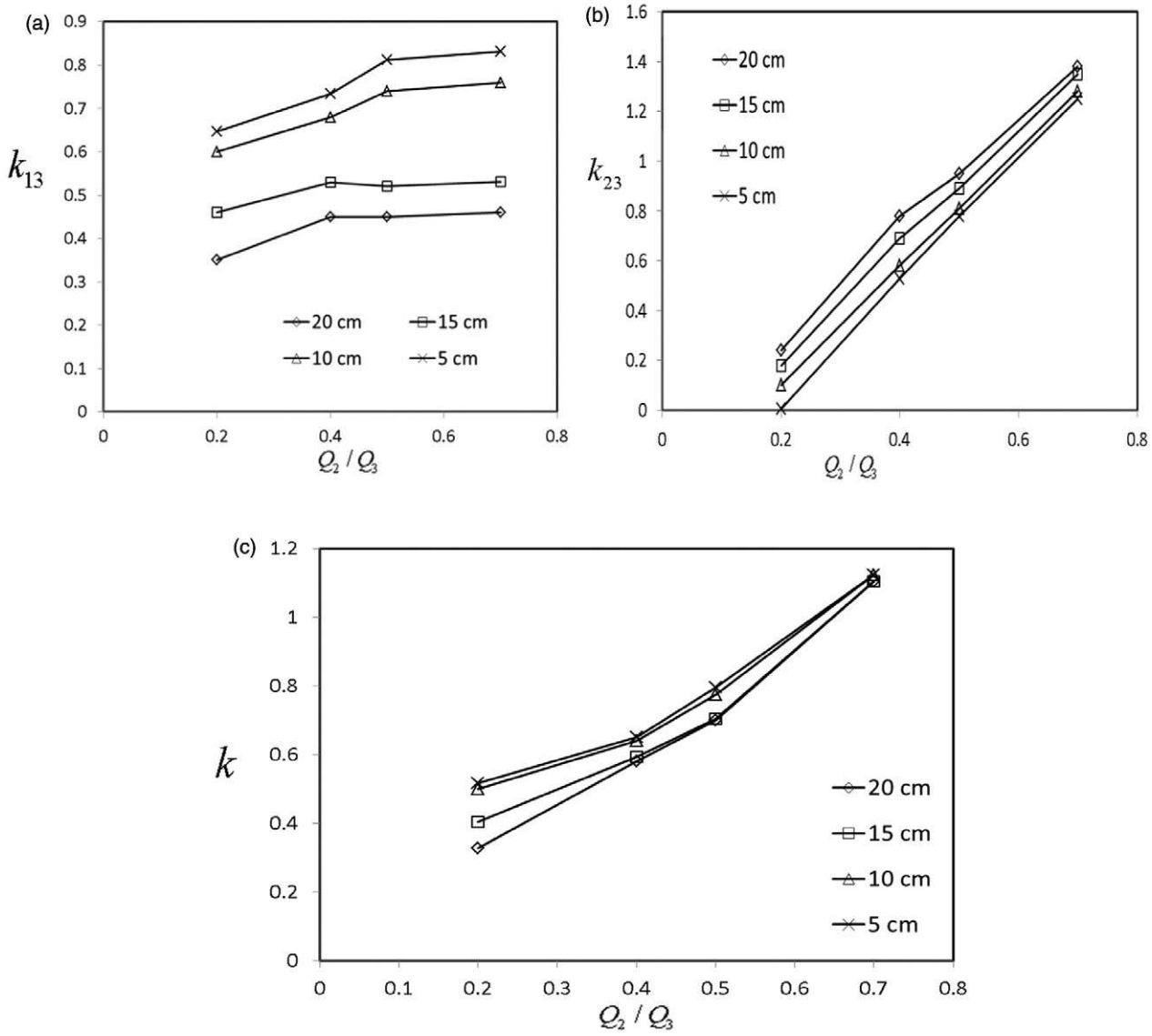

Fig. 9. Energy loss coefficients in the junction chamber for various position of lateral pipe: (a) k_{13}; (b) k_{23}; (c) k.

$D_1 = D_2 = 0.75D_3$ and flow rate ratios of $Q_2/Q_3 = 0$, 0.2, 0.4, 0.5, 0.6, 0.8, 1 at the joint angle of 90. Energy loss coefficients for different flow rate ratios were compared with the experimental results of Wang *et al*. (1998) and physical model of Zhao *et al*. (2006); equation (8) were shown in Figs 11 and 12 for $D_1 = D_2 = 0.75D_3$, $D_1 = 0.75D_3$, $D_2 = 0.5D_3$, respectively. The results show that there is a good agreement between the present simulation with the experimental results of Wang *et al*. (1998) and physical model of Zhao *et al*. (2006). Furthermore, it was shown that the energy loss increases by decreasing the diameter for all flow rates. The flow modelling for the above-mentioned condition was shown in Fig. 13 to investigate the reason.

As shown in this figure, because of the constant flow rate, the velocity increases when diameter decreases. Moreover, the interaction of main and lateral flows increases, which leads to stronger vortical flows. Thus, this will result in increasing the energy loss of flow in manhole.

$$k_{13} = 1 - 2\frac{A_3}{A_1}\left(\frac{Q_1}{Q_3}\right)^2 - 2\frac{A_3}{A_2}\left(\frac{Q_2}{Q_3}\right)^2 \cos\delta + \left(\frac{A_3}{A_1}\right)^2\left(\frac{Q_1}{Q_3}\right)^2 \quad (8)$$

$$k_{23} = 1 - 2\frac{A_3}{A_1}\left(\frac{Q_1}{Q_3}\right)^2 - 2\frac{A_3}{A_2}\left(\frac{Q_2}{Q_3}\right)^2 \cos\delta + \left(\frac{A_3}{A_1}\right)^2\left(\frac{Q_2}{Q_3}\right)^2$$

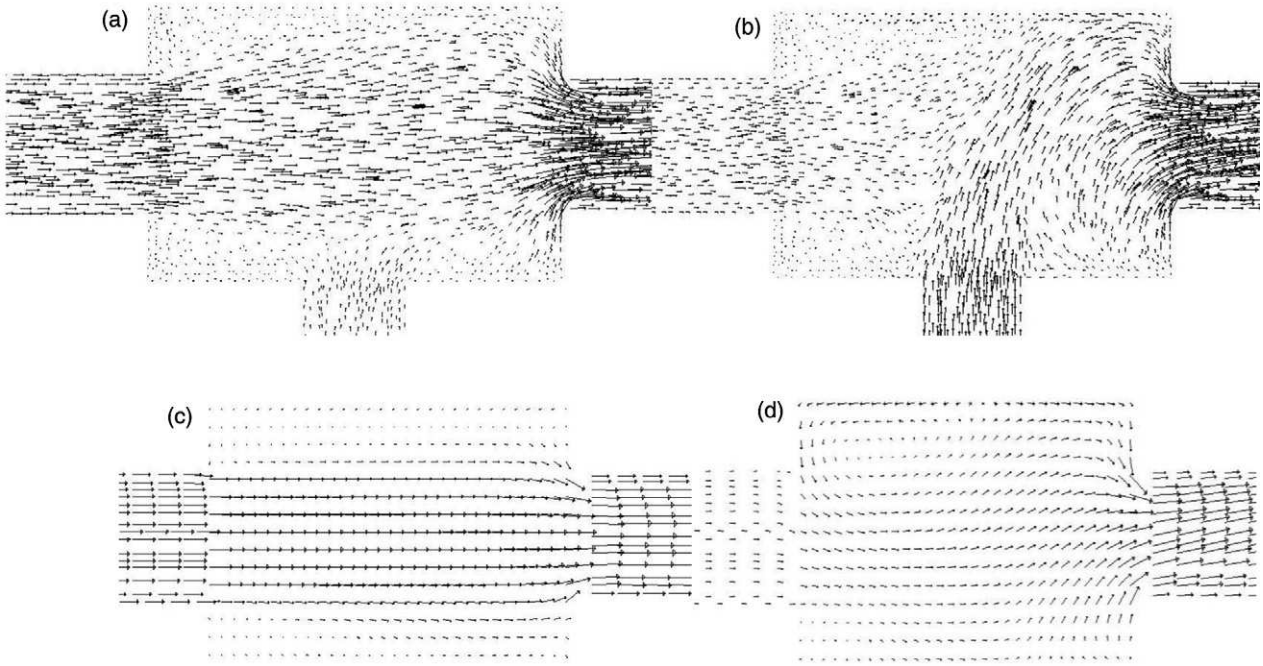

Fig. 10. Velocity vectors inside the junction chamber on the horizontal plane Z/D = 0.8 for different positions of lateral pipe from the bottom of chamber, (a) z = 10 cm, $Q_2/Q_3 = 0.2$; (b) z = 10 cm, $Q_2/Q_3 = 0.7$; (c) z = 20 cm, $Q_2/Q_3 = 0.2$; (d) z = 20 cm, $Q_2/Q_3 = 0.7$. (Arrow length indicates the magnitude of velocity).

$$k = 1 - 2\left(\frac{A_3}{A_1}\right)\left(\frac{Q_1}{Q_3}\right)^2 - 2\left(\frac{A_3}{A_2}\right)\left(\frac{Q_2}{Q_3}\right)^2 \cos\delta + \left(\frac{A_3}{A_1}\right)^2\left(\frac{Q_1}{Q_3}\right)^3 + \left(\frac{A_3}{A_1}\right)^2\left(\frac{Q_2}{Q_3}\right)^3$$

$\delta = \sigma\theta$, where θ is the junction angle and σ is the correction factor. The correction factor, $0 < \sigma < 1$, depends on various parameters, including junction geometry, flow ratios, etc. To simplify our discussion, $\sigma = 8/9$ is assumed for the 90° junction according to Hager (1989), and $\sigma = 1$ for the Edworthy junction. $A_{i=}$ pipe area, with the subscript i = 1, 2 or 3 denoting sections in the straight inlet pipe, the lateral pipe and the outlet pipe, respectively.

Effect of change of longitudinal slope of main and lateral pipes on the hydraulic parameters

In this part, the effect of change in longitudinal slope of main and lateral pipe was investigated on the hydraulic parameters and flow structure. For this purpose, the flow structure was investigated for four different conditions. The slopes of 0.001 and 0.005 were studied for the main pipe. Also, the slopes of 0.01 and 0.02 were studied for the lateral pipe. The results show that pipe slope has no considerable effect on flow modelling and the amount of energy loss in different flow rate ratios (the results were not reported here because of similarity).

Effect of the flow rate in manhole outlet on the hydraulic parameters

In this part, the effect of variation in output flow rate (m^3/s) Q_3 was studied on energy loss and flow modelling. Therefore, flow structure was investigated in four different flow rates, $Q_3 = 0.035$, 0.05, 0.075, 0.1 m3/s, for different ratios of $Q_2/Q_3 = 0.2$, 0.4, 0.5, 0.6, 0.8. Results show that flow rate variations have no considerable effect on flow structure and energy loss. In addition, according to equation (8) (Zhao *et al*. 2006), it was shown that non-dimensional coefficients of energy loss depend only on non-dimensional flow rate ratios Q_2/Q_3, Q_1/Q_3, and are independent of dimensional outflow rate (Q_3) (the results were not reported here because of similarity).

Finally, according to the results of this paper, the following remarks can be considered for the design of sewage systems: **(1)** In circular manholes, for minimum investigated flow rate (ratio $Q_2/Q_3 = 0.2$), the energy loss and the water depth in manhole are 15 and 6% lesser than rectangular shape, respectively. Furthermore, in maximum investigated flow rate (ratio $Q_2/Q_3 = 0.7$), the energy loss and water depth are 5 and 11% lesser than rectangular shape, respectively. Therefore, it is

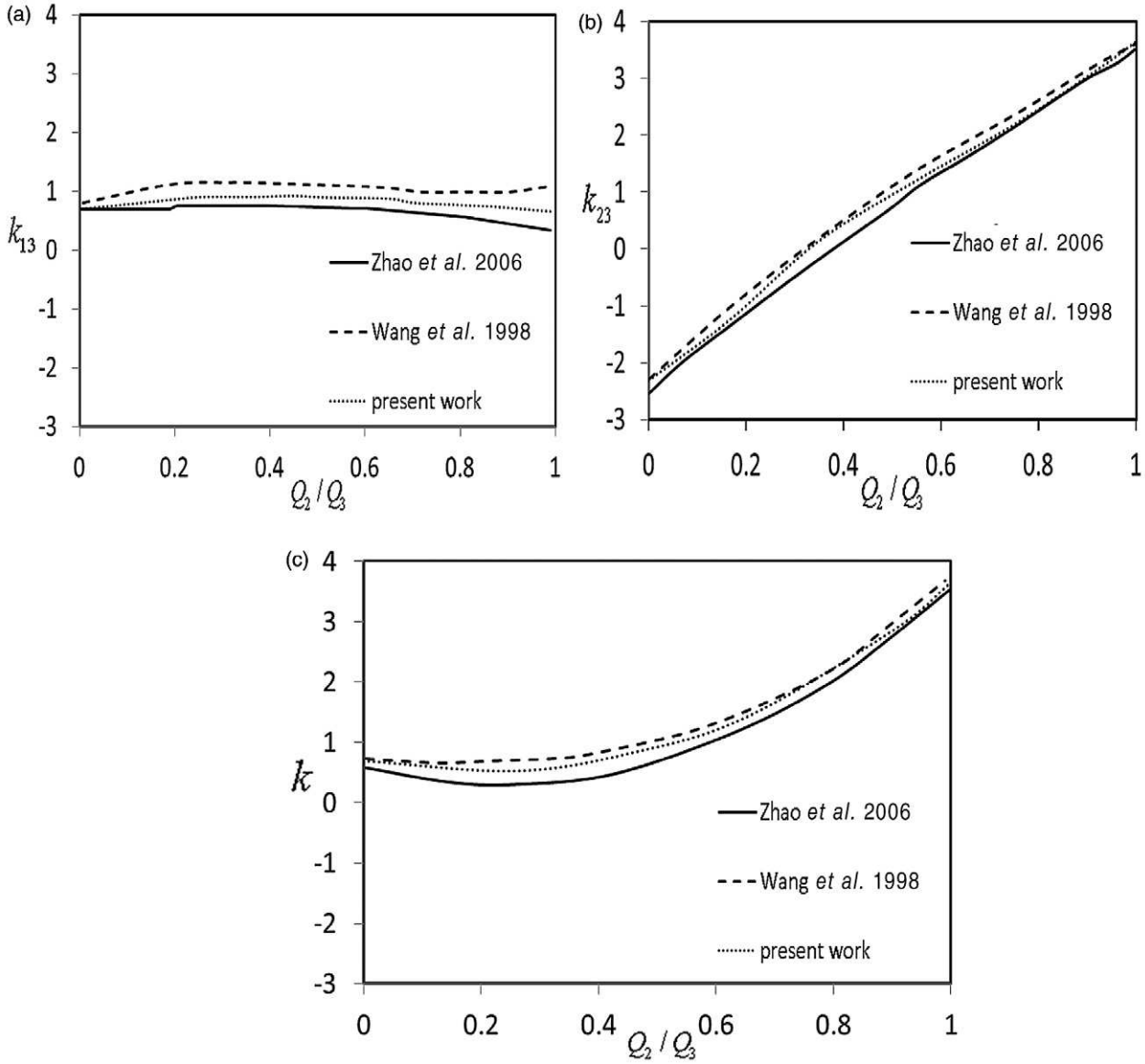

Fig. 11. Energy loss coefficients in the junction chamber for $D_1 = D_2 = 0.75D_3$ (a) k_{13}; (b) k_{23}; (c) k.

preferable to use circular shape manholes instead of rectangular ones.

(2) Increasing the installation position of lateral pipe to manhole causes a decrease in the rate of energy loss in manhole. By increasing the installation position from 5 cm to 20 cm, the energy loss reduced between 1 and 36% in the different flow ratios.

(3) Decreasing the diameter of main and lateral pipes for a constant flow rate leads to increase in the rate of energy loss in manhole. For instance, in flow ratio $Q_2/Q_3 = 1$, when the diameter of pipes is reduced to the half, the value of energy loss in the manhole increases by 13 times.

Conclusion

In the present work, the effects of junction angle of the lateral pipe, and the geometry of the junction chamber on the hydraulic parameters and flow structure, in a fully surcharged sewer junction with a lateral pipe were numerically investigated. Based on the results, the following general conclusions were made:

(1) The PISO algorithm, along with the $k-\omega$ turbulence model, has an adequate performance to predict the energy loss coefficients, and to study flow structures of a junction chamber with a connected lateral pipe.

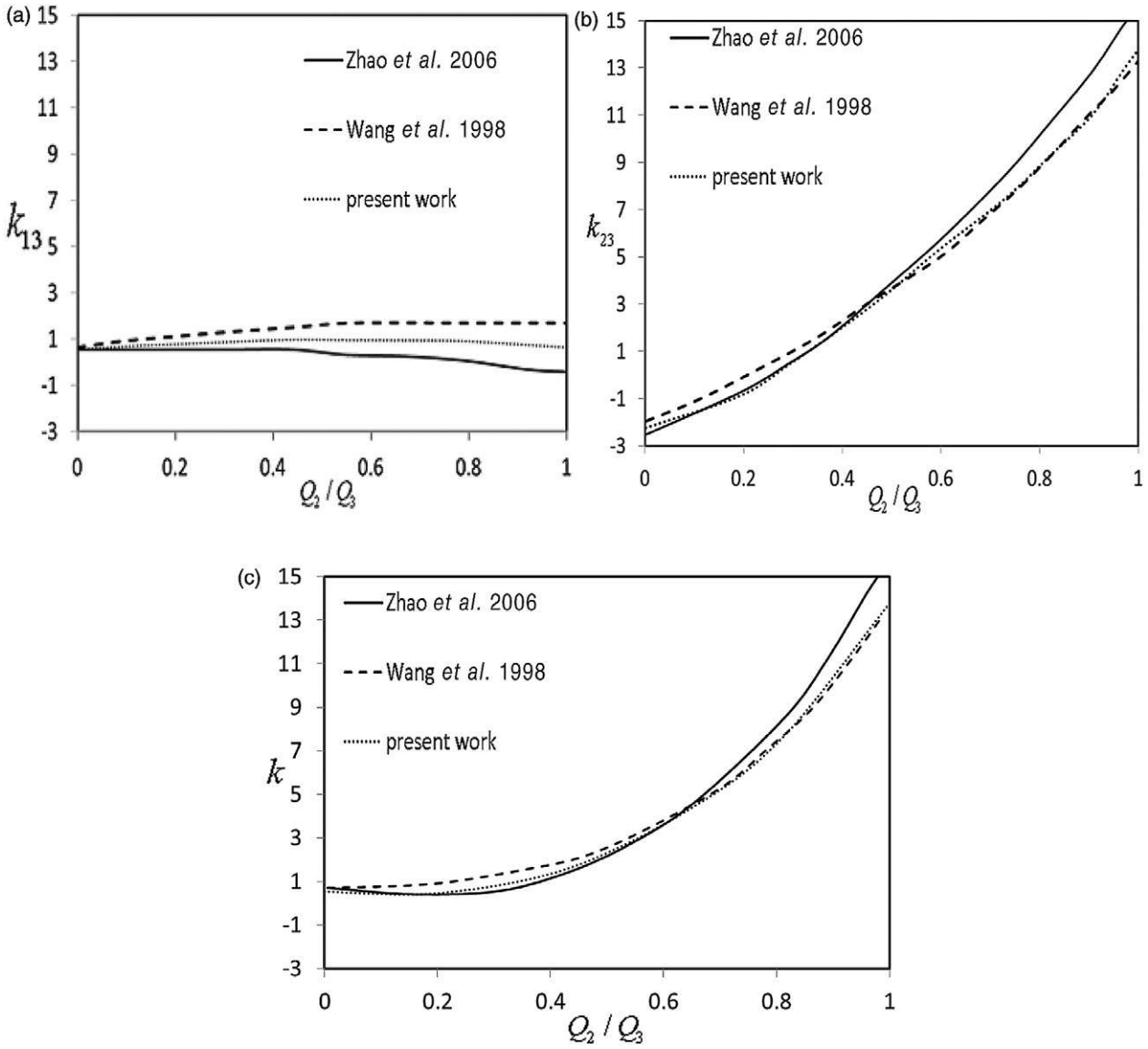

Fig. 12. Energy loss coefficients in the junction chamber for $D_1 = 0.75D_3$, $D_2 = 0.5D_3$ (a) k_{13}; (b) k_{23}; (c) k.

(2) As the ratio of the lateral flow rate to the outlet flow rate (Q_2/Q_3) decreases, at a fixed merge angle, weaker vortical and secondary flows were generated. They are thin and long. As this ratio increases, the vortical flows become more intense, and the flow energy loss and water depth in the junction chamber increase.

(3) At small flow ratios ($\frac{Q_2}{Q_3} < 0.4$), the flow pattern inside the junction chamber does not change considerably with changing lateral pipe merge angle. Thus, the merge angle has little effect on the energy loss coefficients and water depth. On the other hand, at large flow rates ($\frac{Q_2}{Q_3} > 0.6$), increasing the merge angle increases the energy loss coefficients as a larger portion of the flow develops vorticity.

(4) In the junction chamber with circular cross-section, the water depth and energy loss coefficients are less than those in the junction chamber with rectangular cross-section.

(5) Comparing flow structure and energy loss in different installation positions of lateral pipe shows that the rate of energy loss in manhole decreases by heightening the installation position because of a reduction in eddy flows.

(6) The investigation of diameter variation on flow modelling and energy loss revealed that, by decreasing the main and lateral pipes diameters, the rate of energy loss increases because of increasing velocity and eddy flows inside manhole.

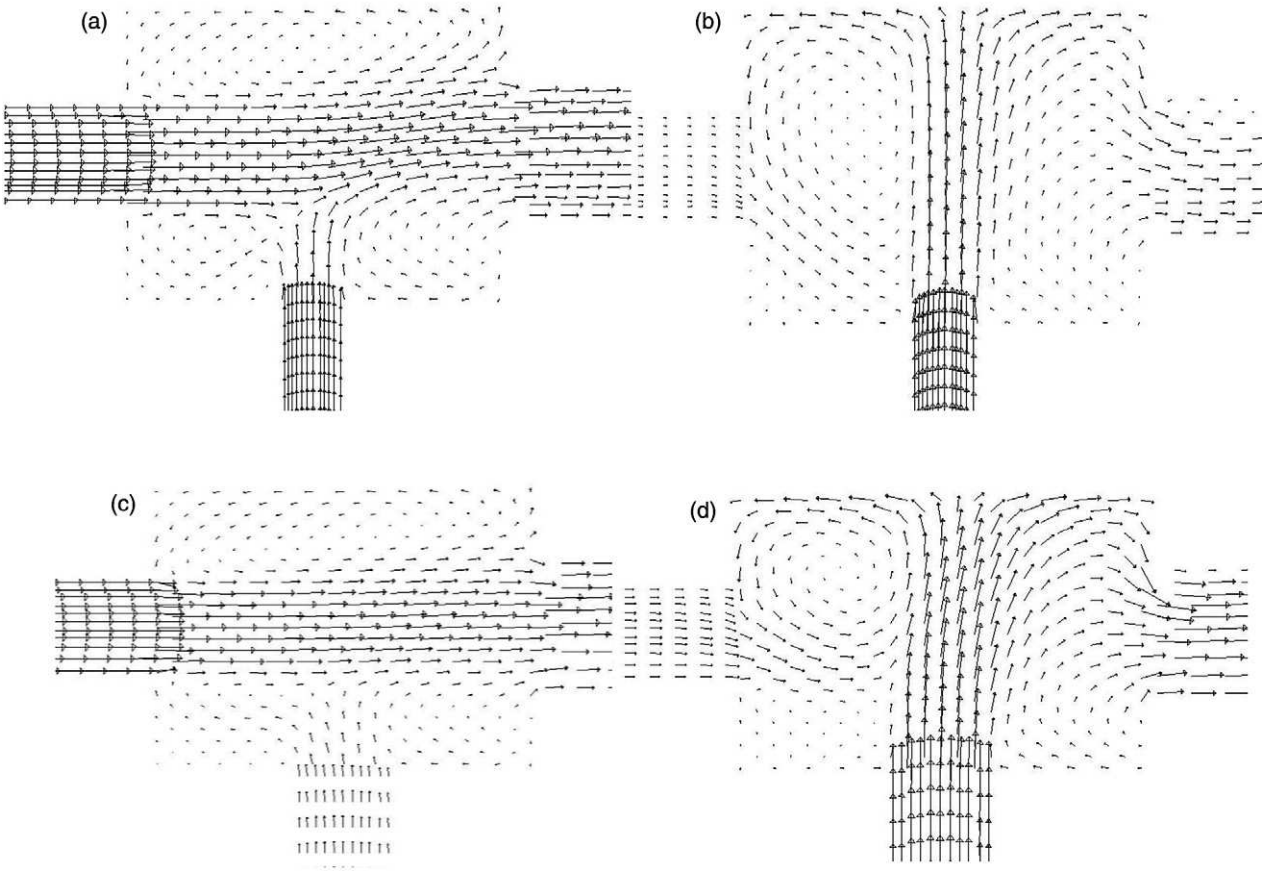

Fig. 13. Velocity vectors inside the junction chamber on the horizontal plane Z/D = 0.8 for (a) $D_1 = 0.75D_3$, $D_2 = 0.5D_3$ $Q_2/Q_3 = 0.2$; (b) $D_1 = 0.75D_3$, $D_2 = 0.5D_3$ $Q_2/Q_3 = 0.7$; (c) $D_1 = D_2 = 0.75D_3$ $Q_2/Q_3 = 0.2$; (d) $D_1 = D_2 = 0.75D_3$ $Q_2/Q_3 = 0.7$. (Arrow length indicates the magnitude of velocity).

(7) Investigating the effect of the slope variation of main and lateral pipe on the rate of energy loss shows that slope variation has no effect on the rate of energy loss.

(8) The comparison between the results of investigating flow modelling for different flow rates (Q_3) shows that the variations of outward flow rate has no considerable effect on flow structure and energy loss for different inward flow rate ratios.

For future works, the flow hydraulics can be investigated under the governing conditions in the joint of two lateral pipes to manhole used in sewage and drainage systems.

To submit a comment on this article, please go to http://mc.manuscriptcentral.com/wej. For further information, please see the Author Guidelines at wileyonlinelibrary.com

References

Ackers, P. (1959) An Investigation of Head Losses at Sewer Manholes. *Civil Eng. Public Works Rev.*, **54** (637), 882–884, 1033–1036.

Anderson, A., Tannehill, J. and Pletcher, R. (1997) *Computational Fluid Mechanics and Heat Transfer*. Taylor & Francis Publishers, Washington, DC.

Bayat, E., Kouchakzadeh, S. and Azimie, R. (2010) Valuating the Carrying Capacity of a Subsurface Drainage Network Based on Spatially Varied Flow Regime. *Irrig. Drain.*, **60** (5), 668–681.

Best, J.L. and Reid, I. (1984) Separation Zone at Open-Channel Junctions. *J. Hydraul. Eng. ASCE*, **110** (112), 1588–1594.

Biron, P., Best, J.L. and Roy, A.G. (1996) Effects of Bed Discordance on Flow Dynamics at Open Channel Confluences. *J. Hydraul. Eng.*, **122** (12), 676–682.

Blaisdell, F.W. and Manson, P.W. (1963) *Loss of Energy at Sharp-Edged Pipe Junction in Water Conveyance Systems*. Technical Bulletin 1283. US Department of Agriculture, Washington, DC.

Del Giudice, G. and Hager, W.H. (2001) Supercritical Flow in 45 Degree Junction Manhole. *J. Irrigat. Drain. Eng. ASCE*, **127** (2), 100–108.

Del Giudice, G., Gisonni, C. and Hager, W.H. (2000) Supercritical Flow in Bend Manhole. *J. Irrigat. Drain. Eng. ASCE*, **126** (1), 48–56.

Gardel, A. (1957a) Les pertes de charge dans les ecoulements au travers de branchments en Te [Pressure Drop in Flows through T-Shaped Pipe Fittings. *Bull. Techn. Suisse Rom.*, **83** (9), 123–130.

Gardel, A. (1957b) Les pertes de charge dans les ecoulements au travers de branchments en Te [Pressure Drop in Flows through

T-Shaped Pipe Fittings]. *Bull. Techn. Suisse Rom.*, **83** (10), 143–148.
Gargano, R. and Hager, W.H. (2002) Supercritical across Sewer Manholes. *J. Hydraul. Eng. ASCE*, **128** (11), 1014–1017.
Gisonni, C. and Hager, W.H. (2002) Supercritical Flow in the Junction. *J. Irrigat. Drain. Eng. ASCE*, **126** (1), 48–56.
Gurram, S.K. and Karki, K.S. (2000) Subcritical Open-Channel Junction Flow. *J. Hydraul. Eng. ASCE*, **126** (1), 87–91.
Guymer, I. and O'Brien, R.T. (2000) Longitudinal Dispersion due to Surcharged Manhole. *J. Hydraul. Eng. ASCE*, **126** (2), 137–149.
Hager, W.H. (1989) Transitional Flow in Channel Junctions. *J. Hydraul. Eng. ASCE*, **115** (2), 243–259.
Hirt, C.W. and Nichols, B.D. (1992) Volume of Fluid (VOF) Method for the Dynamics of Free Boundaries. *J. Comput. Phys.*, **39**, 201–225.
Howarth, D.A. and Saul, A.J. (1984) Energy Loss Coefficients at Manholes. *In* P. Balmer *et al.* (eds). *Proceedings of the Third International Conference on Urban Storm Drainage, Vol. 1*, pp. 127–136. Chalmers University of Technology, Gothenburg, Sweden.
Hsu, C.C., Wu, F.S. and Lee, W.J. (1998a) Flow at 908 Equal-Width Open-Channel Junction. *J. Hydraul. Eng. ASCE*, **124** (2), 186–191.
Hsu, C.C., Lee, W.J. and Chang, C.H. (1998b) Subcritical Open Channel Junction Flow. *J. Hydraul. Eng. ASCE*, **124** (8), 847–855.
Hsu, C.C., Tang, C.J., Lee, W.J. and Shieh, M.Y. (2002) Subcritical 90 Equal-Width Open-Channel Dividing Flow. *J. Hydraul. Eng. ASCE*, **128** (7), 716–720.
Huang, J., Weber, L.J. and Lai, Y.G. (2002) Three-Dimensional Numerical Study of Flows in Open-Channel Junctions. *J. Hydraul. Eng. ASCE*, **128** (3), 268–280.
Ito, H. and Imai, K. (1973) Energy Losses at 90 Degree Pipe Junctions. *J. Hydrol. Div. ASCE*, **99** (9), 1353–1368.
Jasak, H., Weller, H.G. and Gosman, A.D. (1999) High Resolution NVD Differencing Scheme for Arbitrarily Unstructured Meshes. *Int. J. Numer. Methods Fluids*, **31**, 431–449.
Johnston, A.J. and Volker, R.E. (1990) Head Losses at Junction Boxes. *J. Hydraul. Eng. ASCE*, **116** (3), 326–341.
Joy, D.M. and Townsend, R.D. (1981) Improved Flow Characteristics at a 90 Channel Confluence. *In Proceedings of the 5th Canadian Hydrotechnical Conference*, pp. 781–799. Canadian Society for Civil Engineering, National Research Council Press, Ottawa.
Lin, J.D. and Soong, H.K. (1979) Junction Losses in Open-Channel Flows. *Water Resour. Res.*, **15** (2), 414–418.
Lindvall, G. (1984) Head Losses at Surcharged Manholes with A Main Pipe and a Lateral. *In* P. Balmer *et al.* (eds). *Proceedings of the 3rd International Conference on Urban Storm Drainage, Vol. 1*, pp. 137–146. Chalmers University of Technology, Gothenburg, Sweden.
Lindvall, G. (1987) Head Losses at Surcharged Manholes. *In* B.C., Yen (ed). *Urban Storm Water Hydraulics and Hydrology (Joint Proceedings of the 4th International Conference on Urban Storm Drainage and IAHR 22nd Congress)*, pp. 140–141. Water Resources Publications, Highlands Ranch, CO.
Marsalek, J. (1984) Head Losses at Sewer Junction Manholes. *J. Hydraul. Eng. ASCE*, **110** (8), 1150–1154.
Marsalek, J. (1985) *Head Losses at Selected Sewer Manholes*. National Water Research Institute, Canada Centre for Inland Waters, Burlington, Ontario.
McNown, J.S. (1954) Mechanics of Manifold Flow. *Trans. ASCE*, **110**, 1103–1142.
Miller, D.S. (1990) *Internal Flow Systems* (2nd edn). Gulf Publishing Co., Houston, TX.
Ramamurthy, A.S. and Zhu, W. (1997) Combining Flows in Junctions of Rectangular Closed Conduits. *J. Hydraul. Eng. ASCE*, **123** (11), 1012–1019.
Ramamurthy, A.S., Qu, J. and Vo, D. (2007) Numerical and Experimental Study of Dividing Open-Channel Flow. *J. Hydraul. Eng. ASCE*, **113** (10), 1135–1144.
Sakakibari, T., Tanaka, S. and Imaida, T. (1997) Energy Loss at Surcharged Manholes Model Experiment. *Water Sci. Technol.*, **36** (8–9), 65–70.
Sangster, W.M., Wood, H.W., Smerdon, E.T. and Bossy, H.G. (1958) *Pressure Changes at Storm Drain Junctions*. Bulletin No. 41. Engineering Experiment Station, University of Missouri, Columbia, MO.
Sangster, W.M., Wood, H.W., Smerdon, E.T. and Bossy, H.G. (1961) Pressure Changes at Open Junctions in Conduit. *Trans. ASCE*, **126** (Part I), 364–396.
Serre, M., Odgaard, A.J. and Elder, R.A. (1994) Energy Loss at Combining Pipe Junction. *J. Hydraul. Eng. ASCE*, **120** (7), 808–830.
Stein, S.M., Dou, X., Umbrell, E.R. and Jones, J.S. (1999) Storm Sewer Junction Hydraulics and Sediment Transport. Proc., 26th Annual Water Resources Planning and Management Conf, US Federal Highway Administration Turner-Fairbanks Highway Research Centre, VA.
Taylor, E.H. (1944) Flow Characteristics at Rectangular Open-Channel Junctions. *Trans. ASCE*, **109**, 893–912.
Wang, K.H., Cleveland, T.G., Towsley, C. and Umrigar, D. (1998) Energy Loss at Manholes in Surcharged Sewer Systems. *J. Am. Water Resour. Assoc.*, **34** (6), 1391–1400.
Webber, N.B. and Greated, C.A. (1966) An Investigation of Flow Behavior at the Junction of Rectangular Channels. *ICE Proceedings*, **34** (3), 321–334..
Weber, L.J., Schumate, E.D. and Mawer, N. (2001) Experiments on Flow at 90 Open Channel Junction. *J. Hydraul. Eng. ASCE*, **127** (5), 340–350.
Weller, H.G., Tabor, G., Jasak, H. and Fureby, C.A. (1998) Tensorial Approach to Computational Continuum Mechanics Using Object-Oriented Techniques. *Comput. Phys.*, **12**, 620–631.
Yen, B.C. (1986) Hydraulic of Sewers. *In* Yen, B.C. (ed). *Advances in Hydroscience, Vol. 14*, pp. 1–122. Academic Press, New York.
Yen, B.C. and Akan, A.O. (1999) Hydraulic Design of Urban Drainage System. *In* Mays, L.W. (ed). *Hydraulic Design Handbook*, ch. 14. McGraw-Hill Publishing Co, New York.
Zhao, C.H., Zhu, D.Z. and Rajaratnam, N. (2004) Supercritical Sewer Flows at a Combining Junction: A Case Study of Edworthy Trunk Junction, Calgary, Alberta. *J. Environ. Eng. Sci. NRC*, **3** (5), 343–353.
Zhao, C.H., Zhu, D.Z. and Rajaratnam, N. (2006) Experimental Study of Surcharged Flow at Combining Sewer Junctions. *J. Hydraul. Eng.*, **132** (12), 1259–1271.
Zhao, C.H., Zhu, D.Z. and Rajaratnam, N. (2008) Computational and Experimental Study of Surcharged Flow at A 90° Combining Sewer Junction. *J. Hydraul. Eng.*, **134**, 688–700.